

# Transition-State Spectroscopy of Cyclooctatetraene

Paul G. Wenthold, David A. Hrovat, Weston Thatcher Borden,\*  
W. Carl Lineberger\*

The 351-nanometer photoelectron spectrum of the planar cyclooctatetraene radical anion (COT<sup>-</sup>) shows transitions to two electronic states of cyclooctatetraene (COT). These states correspond to the  $D_{4h}$   $^1A_{1g}$  state, which is the transition state for COT ring inversion, and the  $D_{8h}$   $^3A_{2u}$  state. The electron binding energy of the  $^1A_{1g}$  transition state is  $1.099 \pm 0.010$  electron volts, which is lower by  $12.1 \pm 0.3$  kilocalories per mole than that of the  $^3A_{2u}$  state. The photoelectron spectrum shows that the singlet lies well below the triplet in  $D_{8h}$  COT and confirms *ab initio* predictions that the molecule violates Hund's rule. Vibrational structure is observed for both features and is readily assigned by use of a simple potential energy surface.

We report a photodetachment study of the planar cyclooctatetraene radical anion (COT<sup>-</sup>) and the direct observation of the planar transition state for the ring inversion of cyclooctatetraene (COT). Detailed structural and energetic information on the planar transition state for the ring inversion of COT was obtained. This is by far the most complex system for which detailed structural information on a transition state has been experimentally accessible. Our results show that planar, octagonal ( $D_{8h}$ ) COT has a singlet ground state and thus violates Hund's rule.

Until recently, studies of transition states for chemical reactions were carried out indirectly, with the nature of the state inferred from observation of reaction kinetics, isotope and substituent effects, and the stereochemical outcome. Advances in laser technology and spectroscopic techniques have made it possible in certain cases to observe and study transition regions directly (1). Basically, two techniques have been developed for the investigation of transition-state properties. The first involves capturing a bimolecular scattering event in the brief moment during which the reactants pass through the transition region. The second involves the use of either a group of atoms or an electron to fix a complex at a geometry that corresponds to a transition state when the stabilizing feature is removed.

The first examples of transition-state spectroscopy involved the study of metal halide exchange reactions in molecular beam experiments (2). The signatures of

transition states were minor in such experiments, and, at present, most transition-state studies use a departing group or electron. Zewail and co-workers have used photochemical deiodination and decarbonylation to investigate in real-time concertedness in elimination reactions (3) and the nature of tri- and tetramethylene diradicals (4), respectively. The primary difficulty with such measurements is that the departing group may still be associated with the complex during the reaction, which complicates the interpretation of these experiments.

In contrast, when a transition state is accessed by removal of an electron, the nuclei are essentially frozen during the time that the electron is in the neighborhood of the complex. For example, photodetachment of  $\text{FH}_2^-$  leads to formation of  $\text{FH}_2$  at a geometry near the transition state for the reaction of  $\text{F} + \text{H}_2$  (5). Using this technique, Neumark has carried out vibrationally resolved transition-state spectroscopy of small systems (6). Indeed, photodetachment provides a general means for accessing electronic states and regions of potential energy surfaces that cannot be readily studied by other spectroscopic techniques (7). However, all of the previous

transition-state spectroscopy based on the use of this technique and those described above have been restricted to relatively small, simple systems. We now show that it is possible to extend the photodetachment technique to the investigation of the transition state for ring inversion in COT, a large molecule whose electronic structure at planar geometries is of considerable interest.

Planar octagonal ( $D_{8h}$ ) COT has a degenerate ( $e_{2u}$ ) pair of nonbonding molecular orbitals (NBMOs) that are occupied by two electrons. Therefore, Hund's rule (8) predicts that COT should have a triplet ground state ( $^3A_{2u}$ ). However, the two  $e_{2u}$  NBMOs of COT can be chosen so that they have no atoms in common, and qualitative theory (9) predicts that biradicals with disjoint NBMOs will have singlet ground states. Electronic structure calculations (10, 11) provide computational support for the qualitative prediction that  $D_{8h}$  COT will have a singlet ground state ( $^1B_{1g}$ ) and therefore will violate Hund's rule.

Violations of Hund's rule have been predicted (12) and found (13) in tetramethylenbenzene and in other molecules (14) that may be considered to be derivatives of disjoint, non-Kekulé, hydrocarbon diradicals. However, the NBMOs in these non-Kekulé diradicals do not have exactly the same energy, and this nondegeneracy contributes to making the singlet the ground state (14). Consequently, it can be argued that the singlet ground states found for these disjoint diradicals do not constitute violations of the strictest form of Hund's rule.

In contrast to the NBMOs in the non-Kekulé diradicals, the  $e_{2u}$  NBMOs of  $D_{8h}$  COT are degenerate by symmetry. The greater electron correlation in the singlet—a consequence of the nonuniform distribution of electron spins that results from the presence of an alpha spin electron in one disjoint NBMO and a beta spin electron in the other (9)—is wholly responsible for the predicted singlet ground state of  $D_{8h}$  COT. Confirmation that  $D_{8h}$  COT does, in fact, have a singlet ground state is of con-

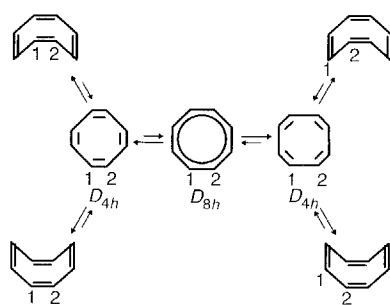
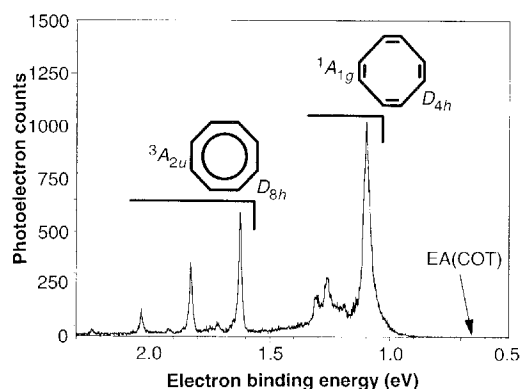


Fig. 1 (left). Ring inversion and bond shifting processes in COT. Fig. 2 (right). Photoelectron spectrum of the cyclooctatetraene radical anion (COT<sup>-</sup>) (351 nm).



P. G. Wenthold and W. C. Lineberger, Jll A and Department of Chemistry and Biochemistry, University of Colorado, and National Institute of Standards and Technology, Boulder, CO 80309, USA.

D. A. Hrovat and W. T. Borden, Department of Chemistry, Box 351700, University of Washington, Seattle, WA 98195, USA.

\*To whom correspondence should be addressed.

siderable importance because it would provide experimental evidence that violations of Hund's rule actually do occur in disjoint diradicals, even when the NBMOs are strictly degenerate.

Experimental verification that  $D_{8h}$  COT has a singlet ground state is challenging. Triplet COT is predicted to have a  $D_{8h}$  equilibrium geometry (10, 11), but earlier attempts to use electron paramagnetic resonance (EPR) to observe this state during triplet-sensitized photolysis of COT (14) or by photodetachment of an electron from COT (15) have failed. The main challenge in showing experimentally that singlet COT is lower in energy than the triplet at planar, octagonal ( $D_{8h}$ ) geometries lies in the fact that the equilibrium geometry of the lowest energy singlet state is nonplanar with alternating single and double carbon-to-carbon bonds (16). Elegant dynamic nuclear magnetic resonance (NMR) experiments, albeit on derivatives of COT, indicate that ring inversion of the  $D_{2d}$  equilibrium geometry of COT has an activation energy of 10 to 11 kcal mol<sup>-1</sup> and that bond shifting in COT requires an additional 3 to 4 kcal mol<sup>-1</sup> (Fig. 1) (17–19).

The proposal of Anet *et al.* (18) that the transition state for ring inversion is planar with alternating single and double carbon-to-carbon bonds ( $D_{4h}$  symmetry) seems to have been generally accepted (16, 19) and is supported by the results of ab initio calculations (10). The  $D_{4h}$  structure results from second-order Jahn-Teller distortion in COT, which splits the  $e_{2u}$  orbitals into non-degenerate  $b_{1u}$  and  $b_{2u}$  orbitals. Although nonplanar transition-state geometries have been proposed for bond shifting in singlet COT (20), multiconfiguration self-consistent field (MCSCF) calculations (10) support Anet's earlier supposition (17, 18) that the transition state for bond shifting in unsubstituted COT is planar with  $D_{8h}$  symmetry. A bond-shifting transition state of lower symmetry cannot be rigorously excluded, but a careful search at the MCSCF(8,8)/6-31G\* level of theory (10) for such a transition state failed to find one, and the calculated barriers to both bond shifting and ring inversion are in excellent agreement with the values from the NMR experiments (17–19).

Photodetachment spectroscopy of COT<sup>-</sup> provides a promising means both for observing the  $D_{4h}$  and  $D_{8h}$  transition states for singlet COT and the lowest  $D_{8h}$  triplet state and for measuring their relative energies. Previous EPR (21), NMR (22), and ultraviolet-visible spectroscopy (15, 23) studies all indicate that COT<sup>-</sup> has a planar geometry in solution, and ab initio calculations indicate a bond-alternated,  $D_{4h}$  geometry in the gas phase as well (24). The tremendous structural difference between the planar  $D_{4h}$  equilibrium geometry

of COT<sup>-</sup> and the nonplanar  $D_{2d}$  geometry of ground-state COT should render transitions from the former to the latter too weak to be observed at energies near the electron affinity (EA), but transitions to planar geometries of the singlet and triplet states of COT are expected to be strong.

In 1979, Brauman and co-workers (25) reported the photodetachment spectrum of COT<sup>-</sup>. The cross section for photodetachment increased slowly above the energy at which photodetachment was first detected ( $0.8 \pm 0.1$  eV), but they did not detect features attributable either to excited vibrational states or to the onset of a second electronic state. The apparent photodetachment threshold energy was well above the adiabatic EA of COT<sup>-</sup> ( $\sim 0.6$  eV), which was previously estimated from thermal electron capture kinetics (26). However, in molecules such as COT where there is a large geometry change between the anion and neutral, accurate determination of the adiabatic EA is difficult for both spectroscopic and kinetic methods (27).

Electron capture by COT in a flowing afterglow ion source cooled with liquid nitrogen formed the COT<sup>-</sup> ions. The 351-nm photoelectron spectrum of COT<sup>-</sup>, obtained with the negative-ion photoelectron spectrometer and experimental protocol described in (7), is shown in Fig. 2. No photoelectrons were observed at electron binding energies near 0.6 eV, the expected EA of COT. However, photodetachment to two distinct electronic states of COT was observed in the spectrum. The lower binding energy feature corresponds to transitions to one electronic state, the intense, asymmetric peak being the origin ( $1.099 \pm 0.010$  eV binding energy) and the three weaker peaks ( $740 \pm 60$ ,  $1315 \pm 40$ , and  $1670 \pm 40$  cm<sup>-1</sup>) corresponding to excited vibrational levels. This feature corresponds to formation of the  $^1A_{1g}$  state of  $D_{4h}$  COT.

The feature at higher binding energy is composed of a vibrational progression with an origin at  $1.624 \pm 0.006$  eV. The vibrations are at  $1635 \pm 20$  cm<sup>-1</sup> (strong) and at  $735 \pm 20$  cm<sup>-1</sup> (weaker). The intensities of the peaks that correspond to the higher frequency vibration indicate a large geometry change along the coordinate for this vibrational mode on going from the equilibrium geometry of COT<sup>-</sup> to that of this upper energy state. We assign this state as  $^3A_{2u}$  of  $D_{8h}$  COT. This method of generating triplet COT from COT<sup>-</sup> in the gas phase is analogous to that of Dvorak and Michl (15), who attempted to observe the  $^3A_{2u}$  state upon photodetachment of matrix-isolated COT<sup>-</sup>.

The photoelectron spectrum of COT<sup>-</sup> can be understood in terms of the schematic diagrams shown in Figs. 3 and 4. The po-

tential energy surfaces for planar COT are shown in Fig. 3. The  $x$  axis for the potential energy surfaces in Fig. 3 is the bond-alternation coordinate, which connects the two different  $D_{4h}$  geometries through a  $D_{8h}$  geometry, where all the C-C bond lengths are equal. The dotted curve, shown for  $^1A_{1g}$ , corresponds to the potential energy along the coordinate for ring inversion, orthogonal to the coordinate for bond alternation. The molecular orbitals for the planar states of COT and their orbital occupancies are shown in Fig. 4. Both the lowest energy

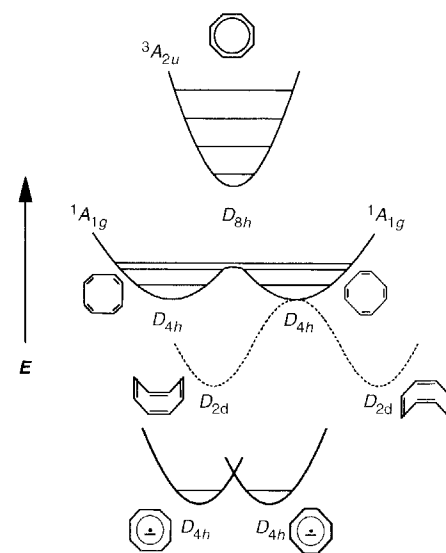


Fig. 3. Schematic potential energy surfaces for COT<sup>-</sup> and for singlet and triplet COT. The  $x$  axis is the "bond-alternation" coordinate for the planar molecule. The  $z$  axis is the out-of-plane bending coordinate, and the potential energy curves for this coordinate are shown with dotted lines.

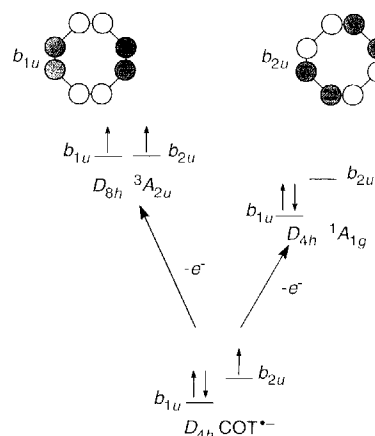


Fig. 4. Top view of the pair of MOs that are occupied in COT<sup>-</sup> and planar COT. The greater occupancy of the  $b_{1u}$  MO in COT<sup>-</sup> and in the  $^1A_{1g}$  state of COT causes these two states to "prefer" bond-alternated,  $D_{4h}$ , geometries, whereas the triplet state "prefers" a geometry where the C-C bond lengths are equal and the  $b_{1u}$  and  $b_{2u}$  orbitals are degenerate.

singlet and triplet surfaces can be accessed upon photodetachment of the  $D_{4h}$   ${}^2B_{2u}$  ion.

It is easiest to analyze the spectrum in Fig. 2 by first considering the higher energy feature, which we assign to the formation of triplet COT. The stronger vibrational progression observed for this state corresponds to the bond alternation vibrational mode of the  ${}^3A_{2u}$  state of  $D_{3h}$  COT. This mode is activated upon detachment of  $D_{4h}$  COT because the equilibrium geometries of COT $^-$  and triplet COT differ along this coordinate (Fig. 3). The differences in the geometries of these species allow the wave function for the lowest vibrational state of COT $^-$  to have significant Franck-Condon overlap with the wave functions for four of the vibrational levels of the  ${}^3A_{2u}$  state of COT.

The observed  $1635\text{-cm}^{-1}$  vibrational frequency agrees well with the value of  $1615\text{ cm}^{-1}$  that was calculated for this mode by the scaling of the MCSCF(8,8)/6-31G\* harmonic frequency by 0.91 to account for anharmonicity and dynamic correlation effects (28). The weaker  $735\text{ cm}^{-1}$  progression is assigned to the symmetric ring-breathing mode, which is calculated to be  $713\text{ cm}^{-1}$ . Not only the positions but also the intensities of the vibrational peaks of the higher energy feature in Fig. 2 are in excellent agreement with those obtained from the use of a modeling procedure (29), in which the Franck-Condon factors were calculated from the MCSCF(8,8)/6-31G\* geometries and frequencies for COT $^-$  and for the  ${}^3A_{2u}$  state of COT.

The lower energy feature in the spectrum is assigned to formation of the  ${}^1A_{1g}$  state of  $D_{4h}$  COT, the transition state for ring inversion. Although this geometry is a saddle point on the singlet potential energy surface, the imaginary frequency at this geometry is computed to be small ( $90i\text{ cm}^{-1}$ ), indicating that the surface is relatively flat in this region. Therefore, the peaks in the spectrum are not excessively broadened (full width at half maximum  $\approx 0.05\text{ eV}$ ) (6).

The first excited vibration at  $740\text{ cm}^{-1}$  can be assigned to the ring-breathing mode, which is calculated to be nearly the same in  ${}^1A_{1g}$  and  ${}^3A_{2u}$ . However, the intense series of vibrational peaks in the band for  ${}^3A_{2u}$ , assigned to the bond alternation mode, are not seen in the band for  ${}^1A_{1g}$ . Instead, we observe a pair of comparatively weak peaks at  $1315$  and  $1670\text{ cm}^{-1}$ .

The scaled MCSCF(8,8)/6-31G\* harmonic vibrational frequency calculated for the bond-alternation mode of the  ${}^1A_{1g}$  state is  $1535\text{ cm}^{-1}$ . However, at  $1535\text{ cm}^{-1}$  ( $4.4\text{ kcal mol}^{-1}$ ), the first excited vibrational level of this mode is expected to be near the top of the barrier at the  $D_{3h}$  transition state for interconversion of the two  $D_{4h}$  geometries (10, 17–19). Thus, as shown schemat-

ically in Fig. 3, the in-phase and out-of-phase combinations of the  $D_{4h}$  vibrational wave functions should be split by an observable amount, and the observed vibrational frequencies of  $1315$  and  $1670\text{ cm}^{-1}$  are assigned to the symmetric and antisymmetric combinations, respectively.

As suggested in Fig. 3, bond alternation is calculated to be slightly greater in the  ${}^1A_{1g}$  state of COT than in COT $^-$ . Therefore, on formation of the  ${}^1A_{1g}$  state of COT from COT $^-$ , some vibrational activity in the bond alternation mode is expected. However, because the  $D_{4h}$  geometry of  ${}^1A_{1g}$  is somewhat closer to the  $D_{4h}$  equilibrium geometry of COT $^-$  than is the  $D_{3h}$  geometry of  ${}^3A_{2u}$ , the peak intensities for transitions from the lowest vibrational level of COT $^-$  to excited vibrational levels of COT are smaller in  ${}^1A_{1g}$  than in  ${}^3A_{2u}$ .

The electron binding energy of the  ${}^1A_{1g}$  state of COT ( $1.099 \pm 0.010\text{ eV}$ ) is  $\sim 0.5\text{ eV}$  greater than the reported  $\sim 0.6\text{ eV}$  EA of the equilibrium geometry of  $D_{2d}$  COT (26). The difference between the electron binding energy of singlet  $D_{4h}$  COT and the adiabatic EA of singlet  $D_{2d}$  COT is equal to the energy difference between the lowest singlet state at these two geometries. Because the  $D_{4h}$   ${}^1A_{1g}$  state of COT is the transition state for ring inversion, the adiabatic EA of COT can be obtained by subtracting the barrier to ring inversion from the  ${}^1A_{1g}$  electron binding energy. The barrier height is estimated to be  $10$  to  $11\text{ kcal mol}^{-1}$  ( $0.43$  to  $0.48\text{ eV}$ ), both by dynamic NMR studies of monosubstituted derivatives of COT (18, 19) and by MCSCF(8,8)/6-31G\* calculations on COT itself (10). Thus, we find  $\text{EA}(\text{COT}) = 0.65\text{ eV}$ , which is close to the estimate of Wentworth and Ristau (26).

The singlet-triplet energy splitting in  $D_{3h}$  COT can be obtained directly from the photoelectron spectrum. The origin of the triplet state is  $0.525 \pm 0.012\text{ eV}$  ( $12.1 + 0.3\text{ kcal mol}^{-1}$ ) above the lowest energy planar ( $D_{4h}$ ) singlet state, and the dynamic NMR studies place the ( $D_{3h}$ ) transition state for bond shifting in singlet COT  $3$  to  $4\text{ kcal mol}^{-1}$  higher in energy than the ( $D_{4h}$ ) transition state for ring inversion (17–19). Combining these values, we estimate that the  $D_{3h}$  singlet state of COT lies  $8$  to  $9\text{ kcal mol}^{-1}$  below the  $D_{3h}$  triplet.

Our best computational estimate of this energy difference, based on calculations that go beyond the MCSCF level and include dynamic electron correlation, is  $\sim 10\text{ kcal mol}^{-1}$  (30). Thus, in addition to predicting qualitatively the violation of Hund's rule in  $D_{3h}$  COT (10), which our photodetachment spectrum of COT $^-$  confirms, ab initio calculations provide an accurate value of the energy by which the  $D_{3h}$  singlet transition

state for bond shifting lies below the  $D_{3h}$  equilibrium geometry of the triplet in COT.

## REFERENCES AND NOTES

1. J. C. Polanyi and A. H. Zewail, *Acc. Chem. Res.* **28**, 119 (1995).
2. P. Arrowsmith *et al.*, *J. Chem. Phys.* **73**, 5895 (1980); P. Arrowsmith, S. H. P. Bly, P. E. Charters, J. C. Polanyi, *ibid.* **79**, 283 (1983); P. R. Brooks, R. I. Curl, T. C. Maguire, *Ber. Bunsenges. Phys. Chem.* **86**, 401 (1982); P. I. Ioring, P. R. Brooks, R. F. Curl Jr., R. S. Judson, R. S. Lowe, *Phys. Rev. Lett.* **44**, 687 (1980); P. R. Brooks, *Chem. Rev.* **88**, 407 (1988).
3. A. H. Zewail, *Femtochemistry—Ultrafast Dynamics of the Chemical Bond* (World Scientific, Teaneck, NJ, 1994).
4. S. Pedersen, J. I. Perek, A. H. Zewail, *Science* **266**, 1359 (1994).
5. D. L. Manolopoulos *et al.*, *ibid.* **262**, 1852 (1993).
6. D. M. Neumark, *Acc. Chem. Res.* **26**, 33 (1993).
7. K. M. Ervin and W. C. Lineberger, in *Advances in Gas Phase Ion Chemistry*, N. G. Adams and L. M. Babcock, Eds. (JAI Press, Greenwich, CT, 1992), vol. 1, pp. 121–166; S. M. Burnett, A. E. Stevens, C. S. Feigerle, W. C. Lineberger, *Chem. Phys. Lett.* **100**, 124 (1983).
8. F. Hund, *Linienpektron Periodisches System der Elemente* (Springer Verlag, Berlin, 1927); *Z. Phys.* **51**, 759 (1928).
9. W. T. Borden and E. R. Davidson, *J. Am. Chem. Soc.* **99**, 4587 (1977); W. T. Borden, in *Diradicals*, W. T. Borden, Ed. (Wiley-Interscience, New York, 1982), pp. 1–72; *Mol. Cryst. Liq. Cryst.* **232**, 195 (1993).
10. D. A. Hrovat and W. T. Borden, *J. Am. Chem. Soc.* **114**, 5839 (1992).
11. M. J. S. Dowar and K. M. Morz, *J. Phys. Chem.* **89**, 4739 (1985).
12. P. M. Lahti, A. S. Ichimura, J. A. Berson, *J. Org. Chem.* **54**, 958 (1989); P. M. Lahti, A. Rossi, J. A. Berson, *J. Am. Chem. Soc.* **107**, 4362 (1985); P. Du *et al.*, *ibid.* **108**, 5072 (1986); D. A. Hrovat and W. T. Borden, *ibid.* **116**, 6327 (1994).
13. J. H. Reynolds *et al.*, *J. Am. Chem. Soc.* **114**, 763 (1992); J. H. Reynolds, J. A. Berson, J. C. Scaiano, A. B. Berinstain, *ibid.*, p. 5866; J. H. Reynolds *et al.*, *ibid.* **115**, 8073 (1993).
14. W. T. Borden, H. Iwamura, J. A. Berson, *Acc. Chem. Res.* **27**, 109 (1994).
15. V. Dvorak and J. Michl, *J. Am. Chem. Soc.* **98**, 1080 (1976).
16. L. A. Paquette, *Tetrahedron* **31**, 2855 (1975); G. I. Fray and R. G. Saxton, *The Chemistry of Cyclooctatetraene and Its Derivatives* (Cambridge Univ. Press, New York, 1978); L. A. Paquette, *Pure Appl. Chem.* **54**, 987 (1982); *Acc. Chem. Res.* **25**, 57 (1992).
17. F. A. L. Anet, *J. Am. Chem. Soc.* **84**, 671 (1962).
18. A. J. R. Bourn, Y. S. Lin, *ibid.* **86**, 3576 (1964).
19. J. F. M. Oth, *Pure Appl. Chem.* **25**, 573 (1971).
20. O. Ermer, F.-G. Klämer, M. Wette, *J. Am. Chem. Soc.* **108**, 4903 (1986); L. A. Paquette, M. P. Trova, J. Luo, A. L. Clough, L. B. Anderson, *ibid.* **112**, 228 (1990); L. A. Paquette *et al.*, *ibid.*, p. 239.
21. T. J. Katz and H. L. Strauss, *J. Chem. Phys.* **32**, 1873 (1960); H. L. Strauss, T. J. Katz, G. K. Fraenkel, *J. Am. Chem. Soc.* **85**, 2360 (1963).
22. T. J. Katz, *J. Am. Chem. Soc.* **82**, 3785 (1960).
23. P. I. Kimmel and H. L. Strauss, *J. Phys. Chem.* **72**, 2813 (1968).
24. J. H. Hammons, D. A. Hrovat, W. I. Borden, *J. Am. Chem. Soc.* **113**, 4500 (1991).
25. R. Gygax, H. L. McPeters, J. I. Brauman, *ibid.* **101**, 2567 (1979).
26. W. E. Wentworth and W. Ristau, *J. Phys. Chem.* **73**, 2126 (1969).
27. M. K. Gilles, K. M. Ervin, J. Ho, W. C. Lineberger, *ibid.* **96**, 1130 (1992).
28. See, for example, J. A. Pople, M. Head-Gordon, D. J. Fox, K. Raghavachari, L. A. Curtiss, *J. Chem.*

- Phys.* **90**, 5622 (1989); J. A. Pople, A. P. Scott, M. W. Wong, L. Radom, *Isr. J. Chem.* **33**, 345 (1993).
29. P. Chen, in *Unimolecular and Bimolecular Reaction Dynamics*, C. Y. Ng, T. Baer, I. Powis, Eds. (Wiley, New York, 1994), pp. 371–425; P. G. Wenthold, M. L. Polak, W. C. Lineberger, *J. Phys. Chem* **100**, 6920 (1996).
30. D. A. Hrovat and W. T. Borden, unpublished results.
31. This research was supported by the National Science Foundation [grants CHE93-18639 (W.C.L.), PHY95-12150 (W.C.L.), and CHE93-14685 (W.T.B.)]. We thank R. F. Gunion and C. F. Logan for assistance with this project and J. Michl for stimulating discussions.

6 March 1996; accepted 17 April 1996